PROCEEDINGS OF SCIENCE

Blazar Studies with CTA

M. Böttcher*
Astrophysical Institute, Department of Physics and Astronomy,
Ohio University, Athens, OH, USA
E-mail: boettchm@ohio.edu

After a brief introduction into the current status of our understanding of γ-ray production in radio-loud AGN, this paper will focus on two aspects in which the anticipated capabilities of the CTA promise progress in our understanding of the location of the gamma-ray emission region in blazars and the mechanisms of γ-ray production. (1) Leptonic and hadronic/lepto-hadronic emission models for blazars predict quite distinct VHE γ-ray spectra and correlated variability features, which CTA will help to distinguish when coordinated with extensive multiwavelength coverage. (2) Near-nuclear IR – optical radiation fields are often invoked for spectral modeling of low-frequency-peaked and intermediate blazars. such radiation fields are expected to leave imprints through $\gamma\gamma$ absorption features and possibly Compton-supported pair cascades. Simultaneous CTA + Fermi observations promise the opportunity to identify the signatures of $\gamma\gamma$ absorption and pair production and thereby provide sringent constraints on the location of the γ-ray production zone.

AGN Physics in the CTA Era - AGN2011,
May 16-17, 2011
Toulouse, France

*Speaker.

PoS(AGN 2011)003

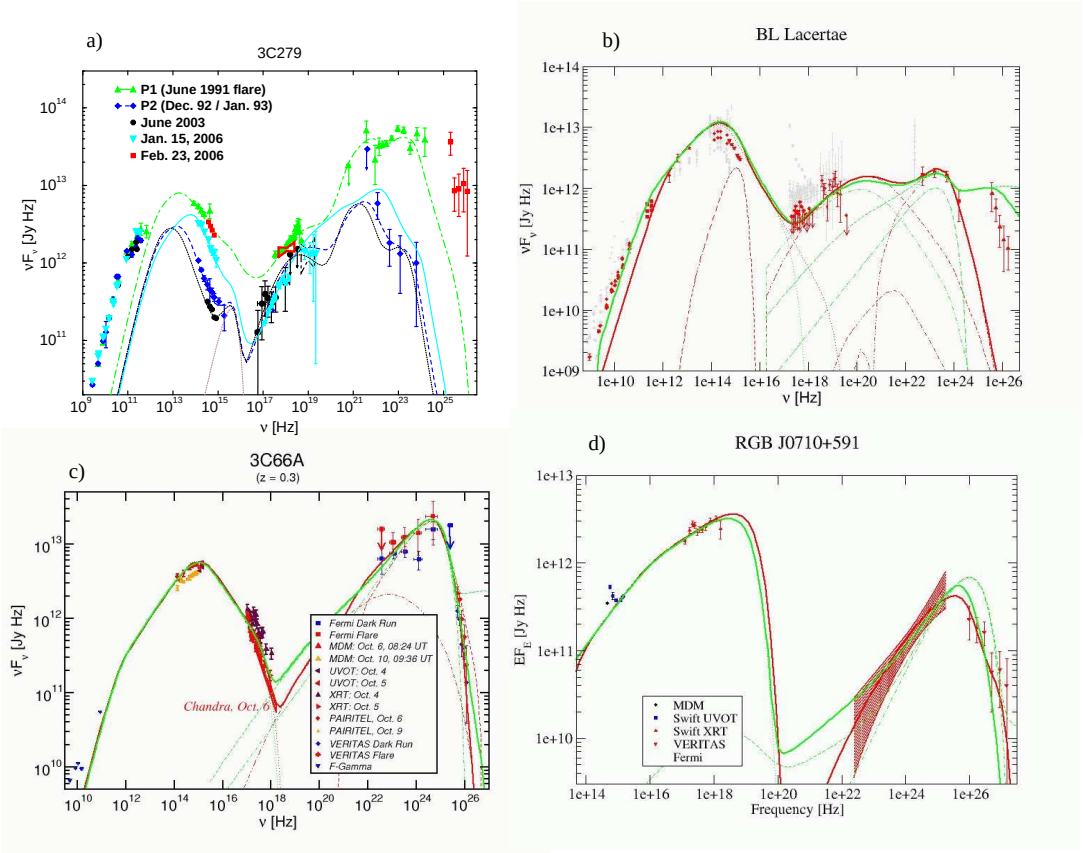

Figure 1: Spectral energy distributions of four sub-classes of blazars: a) the FSRQ 3C279 (from [27]), b) the LBL BL Lacertae, (data from [2]), c) the intermediate BL Lac 3C66A (data from [3]), and d) the HBL RGB J0710+591 (data from [8]). In Panel a) (3C279), lines are one-zone leptonic model fits to SEDs at various epochs shown in the figure. In all other panels, red lines are fits with a leptonic one-zone model; green lines are fits with a one-zone lepto-hadronic model.

1. Introduction

Blazars (BL Lac objects and γ-ray loud flat spectrum radio quasars [FSRQs]) are the most extreme class of active galaxies known. They have been observed at all wavelengths, from radio through very-high-energy (VHE; $E > 100$ GeV) γ-rays. Almost 40 blazars have so far (status: June 2011) been detected as sources of VHE γ-rays by ground-based Cherenkov telescope facilities, and the proposed Cherenkov Telescope Array (CTA) is anticipated to increase the number of known VHE blazars substantially. The broadband continuum spectral energy distributions (SEDs) of blazars are dominated by non-thermal emission and consist of two distinct, broad components: A low-energy component from radio through UV or X-rays, and a high-energy component from X-rays to γ-rays (see, e.g., Figure 1).

Blazars are sub-divided into several types, defined by the location of the peak of the low-energy (synchrotron) SED component, ν_s. Low-synchrotron-peaked (LSP) blazars, consisting of flat-spectrum radio quasars and low-frequency peaked BL Lac objects (LBLs), have $\nu_s \leq 10^{14}$ Hz (i.e., infrared). Intermediate-synchrotron-peaked (ISP) blazars, consisting of LBLs and intermediate BL

Lac objects (IBLs) have $10^{14}\,\mathrm{Hz} < \nu_s \leq 10^{15}$ Hz (i.e., optical – UV), while High-synchrotron-peaked (HSP) blazars, almost all known to be high-frequency-peaked BL Lac objects (HBL), have $\nu_s > 10^{15}$ Hz (i.e., X-rays; [2]). This sequence had first been identified by [32], and was found to be associated with a trend of overall decreasing bolometric luminosity as well as decreasing γ-ray dominance along the sequence FSRQ $\rightarrow$ LBL $\rightarrow$ HBL. According to this classification, the bolometric power output of FSRQs is strongly γ-ray dominated, while HBLs are expected to be synchrotron dominated. However, while the overall bolometric-luminosity trend still seems to hold, recently, even HBLs seem to undergo episodes of strong γ-ray dominance (see, e.g., [12] for an example from a Fermi + H.E.S.S. multiwavelength campaign on PKS 2155-304).

Figure 1 shows examples of blazar SEDs along the blazar sequence, from the FSRQ 3C279 (a), via the LBL BL Lacertae (b) and the IBL 3C 66A (c), to the HBL RGB J0710+591 (d). The sequence of increasing synchrotron peak frequency is clearly visible. However, the Fermi spectrum of the LBL BL Lacertae indicates a γ-ray flux clearly below the synchrotron level, while the SED of the IBL 3C 66A is clearly dominated by the Fermi γ-ray flux, in contradiction with the traditional blazar sequence.

The emission from blazars is known to be variable at all wavelengths. In particular the high-energy emission from blazars can easily vary by more than an order of magnitude between different observing epochs [70, 55, 56]. However, high-energy variability has been observed on much shorter time scales. The most rapid variability has been seen at VHE γ-rays, in some cases down to just a few minutes [10, 13]. The flux variability of blazars is often accompanied by spectral changes. Typically, the variability amplitudes are the largest and variability time scales are the shortest at the high-frequency ends of the two SED components. In HBLs, this refers to the X-ray and VHE γ-ray regimes. Such differential spectral variability is sometimes associated with inter-band or intra-band time lags as well as variability patterns which can be characterized as spectral hysteresis in hardness-intensity diagrams (e.g.,[67, 43, 33, 72]). However, even within the same object this feature tends not to be persistent over multiple observations. Also in other types of blazars, hints of time lags between different observing bands are occasionally found in individual observing campaigns (e.g., [24, 41]), but the search for time-lag patterns persisting throughout multiple years has so far remained unsuccessful (see, e.g., [40] for a systematic search for time lags between optical, X-ray and γ-ray emission in the quasar 3C279).

2. Basic features of leptonic and lepto-hadronic models

The high inferred bolometric luminosities, rapid variability, and apparent superluminal motions provide compelling evidence that the nonthermal continuum emission of blazars is produced in $\lesssim 1$ light day sized emission regions, propagating relativistically with velocity β_Γc along a jet directed at a small angle $\theta_{\rm obs}$ with respect to our line of sight (for details on the arguments for relativistic Doppler boosting, see [61]). Let $\Gamma = (1-\beta_\Gamma^2)^{-1/2}$ be the bulk Lorentz factor of the emission region, then Doppler boosting is determined by the Doppler factor $D = (\Gamma[1-\beta_\Gamma\cos\theta_{\rm obs}])^{-1}$. Let primes denote quantities in the co-moving frame of the emission region, then the observed frequency $\nu_{\rm obs}$ is related to the emitted frequency through $\nu_{\rm obs} = D\,\nu'/(1+z)$, where z is the redshift of the source, and the energy fluxes are connected through $F^{\rm obs}_{\nu_{\rm obs}} = D^3\,F'_{\nu'}$. Intrinsic variability on a co-moving time scale $t'_{\rm var}$ will be observed on a time scale $t^{\rm obs}_{\rm var} = t'_{\rm var}\,(1+z)/D$. Using the latter

transformation along with causality arguments, any observed variability leads to an upper limit on the size scale of the emission region through $R \lesssim c t_{\rm var}^{\rm obs} D/(1+z)$.

While the electron-synchrotron origin of the low-frequency emission is well established, there are two fundamentally different approaches concerning the high-energy emission. If protons are not accelerated to sufficiently high energies to reach the threshold for $p\gamma$ pion production on synchrotron and/or external photons and to contribute significantly to high-energy emission through proton-synchrotron radiation, the high-energy radiation will be dominated by emission from ultra-relativistic electrons and/or pairs (leptonic models). In the opposite case, the high-energy emission will be dominated by cascades initiated by $p\gamma$ pair and pion production as well as proton, $\pi^{\pm}$, and $\mu^{\pm}$ synchrotron radiation, while primary leptons are still responsible for the low-frequency synchrotron emission (lepto-hadronic models). The following sub-sections provide a brief overview of the main radiation physics aspects of both leptonic and lepto-hadronic models.

2.1 Leptonic models

In leptonic models, the high-energy emission is produced via Compton upscattering of soft photons off the same ultrarelativistic electrons which are producing the synchrotron emission. Both the synchrotron photons produced within the jet (the SSC process: [49, 48, 21]), and external photons (the EC process) can serve as target photons for Compton scattering. Possible sources of external seed photons include the accretion disk radiation (e.g., [28, 29]), reprocessed optical – UV emission from circumnuclear material (e.g., the BLR; [63, 19, 36, 30]), infrared emission from a dust torus [20], or synchrotron emission from other (faster/slower) regions of the jet itself [34, 39].

The relativistic Doppler boosting discussed above allows one to choose model parameters in a way that the $\gamma\gamma$ absorption opacity of the emission region is low throughout most of the high-energy spectrum (i.e., low compactness). However, at the highest photon energies, this effect may make a non-negligible contribution to the formation of the emerging spectrum [11] and re-process some of the radiated power to lower frequencies. The resulting VHE γ-ray cut-off and associated MeV – GeV emission features may be revealed by high-resolution, simultaneous Fermi + CTA observations.

Also the deceleration of the jets may have a significant impact on the observable properties of blazar emission through the radiative interaction of emission regions with different speed [34, 38] and a varying Doppler factor [26]. Varying Doppler factors may also be a result of a slight change in the jet orientation without a substantial change in speed, e.g., in a helical-jet configuration (e.g., [69]). In the case of ordered magnetic-field structures in the emission region, such a helical configuration should have observable synchrotron polarization signatures, such as the prominent polarization-angle swing recently observed in conjunction with an optical + Fermi γ-ray flare of 3C 279 [1].

In order to reproduce not only broadband SEDs, but also variability patterns, the time-dependent electron dynamics and radiation transfer problem has to be solved self-consistently. Such time-dependent SSC models have been developed by, e.g., [50, 43, 45, 65]. External radiation fields have been included in such treatments in, e.g., [64, 22, 66].

Leptonic models have generally been very successfully applied to model the SEDs and spectral variability of blazars. The radiative cooling time scales (in the observers's frame) of synchrotron-emitting electrons in a typical $B \sim 1$ G magnetic field are of order of several hours – ~ 1 d at optical

frequencies and $\lesssim$1 hr in X-rays and hence compatible with the observed intra-day variability. However, the recent observation of extremely rapid VHE γ-ray variability on time scales of a few minutes poses severe problems to simple one-zone leptonic emission models. Even with large bulk Lorentz factors of ~ 50, causality requires a size of the emitting region that might be smaller than the Schwarzschild radius of the central black hole of the AGN [18]. As a possible solution, it has been suggested [68] that the γ-ray emission region may, in fact, be only a small spine of ultrarelativistic plasma within a larger, slower-moving jet. Such fast-moving small-scale jets could plausibly be powered by magnetic reconnection in a Poynting-flux dominated jet, as proposed by [35].

2.2 Lepto-hadronic models

If a significant fraction of the jet power is converted into the acceleration of relativistic protons in a strongly magnetized environment, reaching the threshold for $p\gamma$ pion production, synchrotron-supported pair cascades will develop [46, 47]. The acceleration of protons to the necessary ultrarelativistic energies ($E_p^{\rm max} \gtrsim 10^{19}$ eV) requires high magnetic fields of several tens of Gauss to constrain the Larmor radius $R_L = 3.3 \times 10^{15}\, B_1^{-1} E_{19}$ cm, where $B = 10 B_1$ G, and $E_p = 10^{19} E_{19}$ eV, to be smaller than the size of the emission region, typically inferred to be $R \lesssim 10^{16}$ cm from the observed variability time scale. In the presence of such high magnetic fields, the synchrotron radiation of the primary protons [9, 52] and of secondary muons and mesons [58, 52, 53, 54] must be taken into account in order to construct a self-consistent synchrotron-proton blazar (SPB) model. Electromagnetic cascades can be initiated by photons from π^0-decay ("π^0 cascade"), electrons from the $\pi^\pm \to \mu^\pm \to e^\pm$ decay ("$\pi^\pm$ cascade"), p-synchrotron photons ("p-synchrotron cascade"), and μ-, π- and K-synchrotron photons ("$\mu^\pm$-synchrotron cascade").

[53] and [54] have shown that the "π^0 cascades" and "$\pi^\pm$ cascades" from ultra-high energy protons generate featureless γ-ray spectra, in contrast to "p-synchrotron cascades" and"$\mu^\pm$-synchrotron cascades" that produce a two-component γ-ray spectrum. In general, direct proton and $\mu^\pm$ synchrotron radiation is mainly responsible for the high energy bump in blazars, whereas the low energy bump is dominanted by synchrotron radiation from the primary e^-, with a contribution from secondary electrons.

Hadronic blazar models have so far been very difficult to investigate in a time-dependent way because of the very time-consuming nature of the required Monte-Carlo cascade simulations. In general, it appears that it is difficult to reconcile very rapid high-energy variability with the radiative cooling time scales of protons, e.g., due to synchrotron emission, which is $t_{\rm sy}^{\rm obs} = 4.5 \times 10^5\, (1+z)\, D_1^{-1} B_1^{-2} E_{19}^{-1}$ s [9], i.e., of the order of several days for ~ 10 G magnetic fields and typical Doppler factors $D = 10 D_1$. However, rapid variability on time scales shorter than the proton cooling time scale may be caused by geometrical effects.

In order to avoid time-consuming Monte-Carlo simulations of the hadronic processes and cascades involved in lepto-hadronic models, simplified prescriptions of the hadronic processes are often used. [44] have produced analytic fit functions to Monte-Carlo generated results of hadronic interactions using the SOFIA code [51]. Those fits describe the spectra of the final decay products, such as electrons, positrons, neutrinos, and photons from π^0 decay. This approach is appropriate in situations where the decay time scales of pions and muons is much shorter than the synchrotron and Compton cooling time scales of those intermediate products. A more sophisticated method of

evaluating those processes has been presented by [42], who develop template functions for the production spectra of all intermediate species (including pions and muons). Using these, synchrotron and Compton emission of those intermediate particles may be incorporated as well, allowing for the application of this scheme to arbitrarily high magnetic fields and radiation energy densities.

Once the first-generation products are evaluated, one still needs to take into account the effect of cascading, as the synchrotron emission from most of the electrons (and positrons) as well as π^0 decay γ-rays are produced at $\gg$ TeV energies, where the emission region is highly opaque to $\gamma\gamma$ pair production. A quasi-analytical description of those cascades has been developed in [25].

Example model fits to several blazar SEDs using the simplified lepto-hadronic model described in [25] are shown in Fig 1, b) – d) and compared to leptonic models of the same SEDs. As the low-frequency component is electron-synchrotron emission from primary electrons, it is not surprising that virtually identical fits to the synchrotron component can be provided in both types of models. In the high-frequency component, strongly peaked spectral shapes, as, e.g., in 3C 66A and RGB J0710+591 require a strong proton-synchrotron dominance with the cascading of higher-energy ($\gg$ TeV) emission only making a minor contribution to the high-energy emission. This, in fact, makes it difficult to achieve a substantial extension of the escaping high-energy emission into the $>$ 100 GeV VHE γ-ray regime. In objects with a smoother high-energy SED, e.g., BL Lacertae in Fig. 1b, a substantially larger contribution from cascade emission (and leptonic SSC emission) is allowed to account for a relatively high level of hard X-ray / soft γ-ray emission. This also allows for a substantial extension of the γ-ray spectrum into the VHE regime.

Detailed spectral information in the GeV – TeV regime from simultaneous Fermi + CTA observations promise the prospect of identifying the signatures of hadronic processes, such as the spectral flattening towards the highest energies. However, such measurements have to be coordinated with simultaneous multiwavelength coverage at least at optical – X-ray energies, in order to constrain simultaneously the synchrotron and the high-energy components of the SED. The synchrotron SED will yield strict constraints on the underlying electron population (see, e.g., [31]), which can then be used to investigate whether the same electron distribution can be responsible for the X-ray – γ-ray emission, or an additional particle population is required.

3. Internal $\gamma\gamma$ absorption and pair cascades

In the framework of leptonic models, the blazar sequence FSRQ $\rightarrow$ LBL $\rightarrow$ IBL $\rightarrow$ HBL is often modeled through a decreasing contribution of external radiation fields to radiative cooling of electrons and production of high-energy emission [37]. In this sense, HBLs have traditionally been well represented by pure synchrotron-self-Compton models, while FSRQs often require a substantial EC component. This interpretation is consistent with the observed strong emission lines in FSRQs, which are absent in BL Lac objects. At the same time, the denser circumnuclear environment in quasars might also lead to a higher accretion rate and hence a more powerful jet, consistent with the overall trend of bolometric luminosities along the blazar sequence. This may even be related to an evolutionary sequence from FSRQs to HBLs governed by the gradual depletion of the circumnuclear environment [23].

However, in this interpretation, it would be expected that mostly HBLs (and maybe IBLs) should be detectable as sources of VHE γ-rays since in LBLs and FSRQs, electrons are not expected

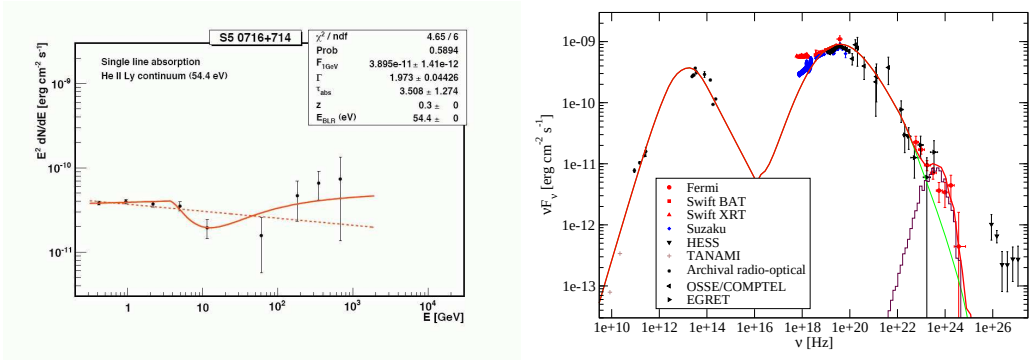

Figure 2: *Left Panel: Fermi* + MAGIC γ-ray spectrum of S5 0716+714. The combined spectrum appears to exhibit a strong absorption trough around 10 – 50 GeV. The solid curve indicates a fit with $\gamma\gamma$ absorption by the HeII recombination continuum. The dashed curve indicates the best fit with a straight power-law [62]. *Right panel:* Fit to the SED of Cen A, including a contribution from deflected pair cascades in the *Fermi* energy range, which substantially improves the fit with plausible model parameters [60].

to reach $\sim$ TeV energies. This appears to contradict the recent VHE γ-ray detections of lower-frequency peaked objects such as W Comae [4], 3C66A [5], PKS 1424+240 [7], BL Lacertae [14], S5 0716+714 [17], and even the FSRQs 3C 279 [15], PKS 1510-089 [71] and PKS 1222+216 (= 4C+21.35; [16]). This suggests that the production of VHE γ-rays is a common phenomenon in all classes of blazars.

The overall SEDs of IBLs detected by VERITAS could still be fit satisfactorily with a purely leptonic model. Fitting the SEDs of the IBLs 3C66A and W Comae with a pure SSC model, while formally possible, would require rather extreme parameters. In particular, magnetic fields several orders of magnitude below equipartition would be needed, which might pose a severe problem for jet collimation. Much more natural fit parameters can be adopted when including an EC component with an infrared radiation field as target photons [6, 3]. In the lower-frequency peaked LBLs and, in particular, FSRQs, the presence of rather high-luminosity circum-nuclear radiation fields is clearly established. This poses a problem for the escape of VHE γ-rays as they will be absorbed through $\gamma\gamma$ pair production on these near-nuclear radiation fields.

The tell-tale signature of such internal $\gamma\gamma$ absorption would be absorption troughs. If the circumnuclear radiation field is dominated by Lyα emission, the resulting $\gamma\gamma$ absorption trough is expected to be centered around $E_\gamma \sim (m_e c^2)^2/(E_{\rm target}\,[1+z]) \sim 25/(1+z)$ GeV. Unfortunately, this places the absorption features from circumnuclear radiation fields dominated by broad-line region (BLR) emission right at the transition between the energy range accessible by *Fermi* and the VHE γ-rays accessible by ground-based Cherenkov telescope facilities. Higher-ionization signatures, in particular from He II, may produce absorption features extending down to $\sim$ a few GeV, and the combined absorption features from He II plus lower-energy emission lines from the BLR have been invoked by [57] to explain the spectral breaks in the *Fermi* spectra of several low-frequency peaked blazars.

While the *Fermi* spectral breaks may be a tantalizing hint towards the importance of internal $\gamma\gamma$ absorption on near-nuclear radiation fields, the ultimate proof would come from the observation of the up-turn towards higher energies, beyond the $\gamma\gamma$ absorption trough. A comprehensive, combined

analysis of *Fermi* + ground-based VHE γ-ray observations of several VHE γ-ray blazars has been peformed by [62]. In a few cases, the expected absorption trough features, including the recovery of the flux towards VHE γ-rays have been found in this analysis. Figure 2a shows the *Fermi* + MAGIC γ-ray spectrum of the LBL S5 0716+714, which constitutes one of the strongest cases for the existence of a $\gamma\gamma$ absorption trough. However, a severe caveat in this analysis is that in most cases, the *Fermi* and VHE measurements were not simultaneous, and the *Fermi* spectra were obtained over substantially longer integration times than the VHE γ-ray ones. Therefore, mismatches in the simultaneous spectral shapes or normalizations may conceivably yield artificial structures which may be mis-interpreted as $\gamma\gamma$ absorption troughs.

If the VHE γ-ray production in low-frequency peaked VHE blazars occurs within the influence of strong circum-nuclear radiation fields, $\gamma\gamma$ absorption and pair production will lead to the development of Compton-supported pair cascades. It has been shown in [59] that even very weak ($B \lesssim \mu$G) magnetic fields can efficiently deflect those cascades and lead to observable off-axis cascade emission peaking in the *Fermi* energy range. This may explain the GeV γ-ray fluxes observed by EGRET and *Fermi* from several radio galaxies. Figure 2b shows an example of the fit to the SED of Cen A, where an off-axis cascade contribution in the *Fermi* energy range allows for a satisfactory representation of the *Fermi* spectrum with reasonable parameters as expected from misaligned blazars [60].

Acknowledgments

This work has been supported by NASA through Fermi Guest Investigator Grants NNX09AT81G, NNX09AT82G, NNX10AO49G and Astrophysics Theory Program grant NNX10AC79G.

References

[1] Abdo, A. A., et al., 2010, Nature, 463, 919

[2] Abdo, A. A., et al., 2010b, ApJ, 716, 30

[3] Abdo, A. A., et al., 2011, ApJ, 726, 43

[4] Acciari, V. A., 2008, ApJ, 684, L73

[5] Acciari, V. A., 2009a, ApJ, 693, L104

[6] Acciari, V. A., 2009b, ApJ, 707, 612

[7] Acciari, V. A., et al., 2010a, ApJ, 708, L100

[8] Acciari, V. A., et al., 2010b, ApJ, 715, L49

[9] Aharonian, F. A., 2000, New Astron., 5, 377

[10] Aharonian, F. A., et al., 2007, ApJ, 664, L71

[11] Aharonian, F. A., Khangulyan, D., & Costamante, L., 2008, MNRAS, 387, 1206

[12] Aharonian, F. A., et al., 2009, A&A, 502, 749

[13] Albert, J., et al., 2007a, ApJ, 669, 862

[14] Albert, J., et al., 2007b, ApJ, 66, L17

[15] Albert, J., et al., 2008, Science, 320, 1752

[16] Aleksic, J., et al., 2011, ApJ, 730, L8

[17] Anderhub, H., et al., 2009, ApJ, 704, L129

[18] Begelman, M. C., Fabian, A. C., & Rees, M. J., 2008, MNRAS, 384, L19

[19] Blandford, R. D., & Levinson, A., 1995, ApJ, 441, 79

[20] Blażejowski, M., et al., 2000, ApJ, 545, 107

[21] Bloom, S. D., & Marscher, A. P., 1996, 461, 657

[22] Böttcher, M., & Chiang, J., 2002, ApJ, 581, 127

[23] Böttcher, M., & Dermer, C. D., 2002, ApJ, 564, 86

[24] Böttcher, M., et al., 2007, ApJ, 670, 968

[25] Böttcher, M., 2010, in proc. "Fermi Meets Jansky", Bonn, Germany, 2010, Eds.: T. Savolainen, E. Ros, R. W. Porcas, & J. A. Zensus; p. 41

[26] Böttcher, M., & Principe, D., 2009, ApJ, 692, 1374

[27] Collmar, W., et al., 2010, A&A, 522, A66

[28] Dermer, C. D., Schlickeiser, R., & Mastichiadis, A., 1992, A&A, 256, L27

[29] Dermer, C. D., & Schlickeiser, R., 1993, ApJ, 416, 458

[30] Dermer, C. D., Sturner, S. J., & Schlickeiser, R., 1997, ApJS, 109, 103

[31] Finke, J. D., Dermer, C. D., & Böttcher, M., 2008, ApJ, 686, 181

[32] Fossati, G., et al., 1998, MNRAS, 299, 433

[33] Fossati, G., et al., 2000, ApJ, 541, 166

[34] Georganopoulos, M., & Kazanas, D., 2003, ApJ, 594, L27

[35] Giannios, D., Uzdensky, D. A., & Begelman, M. C., 2009, MNRAS, 395, L29

[36] Ghisellini, G., & Madau, P. 1996, MNRAS, 280, 67

[37] Ghisellini, G., et al., 1998, MNRAS, 301, 451

[38] Ghisellini, G., Tavecchio, F., & Chiaberge, M., 2005, A&A, 432, 401

[39] Ghisellini, G., & Tavecchio, F., 2008, MNRAS, 386, L28

[40] Hartman, R. C., et al., 2001, ApJ, 558, 583

[41] Horan, D., et al., 2009, ApJ, 695, 596

[42] Hümmer, S., et al., 2010, ApJ, 721, 630

[43] Kataoka, J., et al., 2000, ApJ, 528, 243

[44] Kelner, S. R., & Aharonian, F. A., 2008, Phys. Rev. D., 78, 034013

[45] Li, H., & Kusunose, M., 2000, ApJ, 536, 729

[46] Mannheim, K., & Biermann, P. L., 1992, A&A, 253, L21

[47] Mannheim, K., 1993, A&A, 221, 211

[48] Maraschi, L., Celotti, A., & Ghisellini, G., 1992, ApJ, 397, L5

[49] Marscher, A. P., & Gear, W. K., 1985, ApJ, 298, 114

[50] Mastichiadis, A., & Kirk, J. G., 1997, A&A, 320, 19

[51] Mücke, A., et al., 2000, Comp. Phys. Comm., 124, 290

[52] Mücke, A., & Protheroe, R. J., 2000, AIP Conf. Proc., 515, 149

[53] Mücke, A., & Protheroe, R. J., 2001, Astropart. Phys., 15, 121

[54] Mücke, A., et al., 2003, Astropart. Phys., 18, 593

[55] Mukherjee, R., et al., 1997, ApJ, 490, 116

[56] Mukherjee, R., et al., 1999, ApJ, 527, 132

[57] Poutanen, J., & Stern, B., 2010, ApJ, 717, L118

[58] Rachen, J., & Mészáros, P., 1998, Phys. Rev. D, 58, 123005

[59] Roustazadeh, P., & Böttcher, M., 2010, ApJ, 717, 468

[60] Roustazadeh, P., & Böttcher, M., 2011, ApJ, 728, 134

[61] Schlickeiser, R., 1996, A&AS, 120, 481

[62] Şentürk, G. D., et al., 2011, in preparation

[63] Sikora, M., Begelman, M., & Rees, M. 1994, ApJ, 421, 153

[64] Sikora, M., et al., 2001, ApJ, 554, 1

[65] Sokolov, A., Marscher, A. P., & McHardy, I. A., 2004, ApJ, 613, 725

[66] Sokolov, A., & Marscher, A. P., 2005, ApJ, 629, 52

[67] Takahashi, T., et al., 1996, ApJ, 470, L89

[68] Tavecchio, F., & Ghisellini, G., 2008, MNRAS, 385, L98

[69] Villata, M., & Raiteri, C. M., 1999, A&A, 347, 30

[70] von Montigny, C., et al., 1995, ApJ, 440, 525

[71] Wagner, S., & Behera, B., 2010, 10th HEAD Meeting, Hawaii (BAAS, 42, 2, 07.05)

[72] Zhang, Y. H., et al., 2002, ApJ, 572, 762